

Colloidal fibers as structurant for worm-like micellar solutions

Giuliano Zanchetta^{1,2} · Shadi Mirzaagha³ · Vincenzo Guida⁴ · Fabio Zonfrilli⁴ · Marco Caggioni⁵ · Nino Grizzuti³ · Rossana Pasquino³ · Veronique Trappe¹

Abstract

We investigate the rheological properties of a simplified version of a liquid detergent composed of an aqueous solution of the linear alkylbenzene sulphonate (LAS) surfactant, in which a small amount of fibers made of hydrogenated castor oil (HCO) is dispersed. At the concentration typically used in detergents, LAS is in a worm-like micellar phase exhibiting a Maxwellian behavior. The presence of HCO fibers provides elastic properties, such that the system behaves as a simple Zener body, mechanically characterized by a parallel connection of a spring and a Maxwell element. Despite this apparent independence of the contributions of the fibers and the surfactant medium to the mechanical characteristics of the system, we find that the low frequency modulus increases with increasing LAS concentration. This indicates that LAS induces attractive interactions among the HCO fibers, resulting in the formation of a stress-bearing structure that withstands shear at HCO concentrations, where the HCO fibers in the absence of attractive interactions would not sufficiently overlap to provide stress-bearing properties to the system.

Keywords Colloidal fiber · Gel · Depletion · Worm-like micelle · Rheology

Introduction

Liquid detergents are generally based on aqueous solutions of surfactant that form, depending on surfactant concentration, temperature and pH, various micellar phases, such as spherical and wormlike micelles or lamellar bilayers [1, 2]. The transition from one phase to another can often be induced by a small variation in composition or temperature, which in turn leads to

dramatic changes in the rheological response of the system [3]. However, even though the relaxation times can vary by orders of magnitude, surfactant systems generally do not possess a yield stress.

To fulfill the requirements of modern detergents, yield stress properties are nonetheless often desired to prevent creaming or sedimentation of capsules and particles. One of the strategies used to provide such solid-like properties is to add a small amount of colloidal fibers to the detergent base. Indeed, rod-like colloids or semi-flexible polymers with large aspect ratios can form entangled networks, spanning the whole system at very low number concentration, such that they can be used to efficiently modify the mechanical properties of fluids [4]. Prominent examples of fiber networks in nature are those formed by semi-flexible polymers like actin [5], which has been widely investigated and modeled [6]. Typical fiber-based rheology modifiers in industrial products include acrylic polymers [7], gums [8], and polysaccharides like cellulose derivatives [9]. New systems are constantly explored, such as nano-fibrils of cellulose that have recently gained interest because of their high moduli, easy surface modification, and sustainable production [10]. The behavior of systems containing fibers can vary widely, depending on the physical and chemical properties of the fibers. By tuning for instance the size or the flexibility of the rods, it is possible

Giuliano Zanchetta and Shadi Mirzaagha contributed equally to this work.

✉ Rossana Pasquino
r.pasquino@unina.it

¹ Department of Physics, University of Fribourg, Fribourg, Switzerland

² Department of Medical Biotechnology and Translational Medicine, University of Milano, Milan, Italy

³ Department of Chemical, Materials and Industrial Production Engineering, Università degli Studi di Napoli Federico II, Naples, Italy

⁴ Bruxelles Innovation Center, Procter & Gamble Co., Strombeek Bever, Belgium

⁵ Microstructured Fluids Group, Procter & Gamble Co., West Chester, OH, USA

to tune the properties of the dispersions. Already at low volume fraction, systems containing rod-like particles show a rich behavior, which is interesting both from a scientific and technological point of view: birefringence and elasticity are only two examples of the phenomena that have been observed [11–13].

In this paper, we characterize the rheological behavior of a simplified version of a commercial liquid detergent. The system is composed of colloidal fibers that are suspended in an aqueous solution of entangled micelles [14]. One peculiarity of this system is that the fibers are directly crystallized in the surfactant solution, such that the surfactant forming the continuous phase of the system is also the stabilizing agent. Previous investigations have focused on the effect of crystal morphology in samples with high surfactant concentration [14, 15]. Here, we explore how the interplay between the structuring fiber network and the viscoelastic surfactant solution affects the overall mechanical properties of the system by investigating the rheological properties of samples with varying surfactant and fiber concentrations in oscillatory and steady shear experiments.

Materials and methods

Sample preparation

The systems investigated are composed of aqueous solutions of linear alkylbenzene sulphonate (LAS), neutralized with monoethanolamine (MEA) to pH = 8, and hydrophobic fibers made of hydrogenated castor oil (HCO). The HCO-fibers were produced by emulsion crystallization of HCO in a solution of LAS at a concentration of [LAS] = 16 wt%. In this process, HCO is emulsified at elevated temperature and the emulsion is slowly cooled while sheared. During cooling, HCO nucleates within the aqueous surfactant phase and the emulsions droplets act as a reservoir for HCO in the aqueous phase [16]. The actual shape of the HCO-crystallites resulting from this production method sensitively depends on the cooling rate and shear rate used. Three main crystal morphologies have been reported: irregular crystals, rosettes, and fibers [14, 15]. In this paper, we explore the behavior of suspensions containing mainly rigid fibers with diameters of ~ 20 nm and widely varying lengths (2–20 μm) [14]. The density of the fibers essentially matches the density of the surfactant phase, such that gravity effects are negligible. Samples with LAS concentrations ranging from 1.6 to 16 wt% and HCO concentrations ranging from 0.01 to 4 wt% are prepared by dilution from a stock solution containing [HCO] = 4 wt% and [LAS] = 16 wt%. For reference, we additionally prepare a concentration series of LAS without HCO. All starting materials were kindly provided by Procter & Gamble.

Rheology

Rheological tests are performed with commercial rheometers (MCR 502 and MCR 702, Anton Paar) using a cone and plate geometry with a cone radius of 25 mm and a cone angle of 1° . The temperature is controlled to 20°C by Peltier elements and evaporation is minimized by using a solvent trap. A fresh sample is loaded for each experiment, and reproducibility is checked by repeating the same test three times. Prior to all oscillatory shear experiments, the samples are presheared at a shear rate of 100 s^{-1} for 100 s and then left to rest for 100 s, where we made sure that a 100 s resting period was sufficient to warrant a reproducible and almost stationary behavior. Small amplitude oscillatory shear experiments are performed with strains of 0.1–0.5%, ensuring that the measurements are in the linear viscoelastic regime. The viscoelastic properties are measured in the frequency range $\omega = 1\text{--}100$ rad/s. Steady-shear tests are performed by decreasing the strain rate from 100 to 10^{-5} s^{-1} . The flow curve tests are performed by using logarithmically increasing sampling times, ensuring steady state conditions at all shear rates. That slip is not significant in our experiments has been verified by using various shear geometries, including couette, plate/plate, and cone/plate geometries with different cone angles; we found that the mechanical response of our system is independent of the geometry used.

Results and discussion

To assess the mechanical properties of our multicomponent system, composed of a surfactant solution and HCO colloidal fibers, we first consider the mechanical response of the surfactant solution. We determine the low shear viscosity η_0 of LAS solutions with varying LAS-concentrations at $T = 20^\circ\text{C}$ in shear rate experiments. As shown in Fig. 1, η_0 is a strong function of LAS concentration, [LAS]. For [LAS] < 5 wt%, the viscosity increases slowly with [LAS] to then increase by more than three orders of magnitude within the concentration range of 5–13 wt%. Such concentration dependence of the viscosity has been observed in numerous other surfactant systems [3, 17–19], and is generally assigned to the formation of worm-like micelles that increase in length as the concentration is increased, thereby becoming strongly entangled. Stress relaxation is here determined by breakage and reptation, the faster of the two processes being that determining the relaxation time of the system [20]. In the worm-like micellar phases of LAS, breakage is dominating; this is evidenced by a frequency dependence of the storage and loss modulus that is well-described by the Maxwell model.

As an example, we show in Fig. 2a the response obtained for [LAS] = 13 wt%; as typically found for Maxwellian fluids, the storage G' and loss modulus G'' increase respectively with ω^2 and ω . Beyond [LAS] = 13 wt%, we find that the low shear

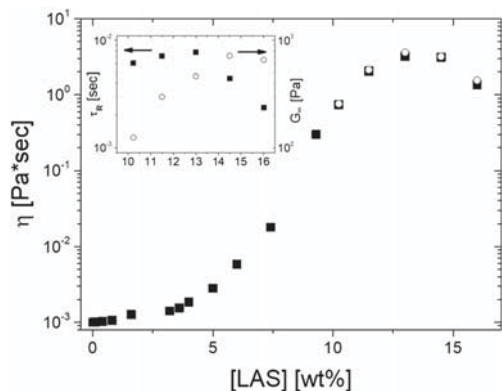


Fig. 1 Zero-shear viscosity for LAS solutions at $T=20$ °C (black squares). Inset: LAS-concentration dependence of relaxation time (left axis) and high frequency elastic modulus (right axis) obtained from Maxwell fits of the frequency dependence of G' and G'' . The product $G_\infty \times \tau_R$ is shown as open circles in the main panel

viscosity decreases again. An analysis of the frequency dependent moduli, using the Maxwell model to fit the data obtained at different LAS-concentrations, reveals that the origin of this decrease is mainly due to a pronounced decrease of the relaxation time beyond $[LAS] = 13$ wt%. This is shown in the inset of Fig. 1, where we display the concentration dependence of both the relaxation time τ_R and the high frequency modulus G_∞ obtained for $[LAS] = 10\text{--}16$ wt%; to demonstrate the consistency between the data obtained in oscillatory shear experiments and those obtained in steady shear rate experiments, we report $\eta_0 = G_\infty \times \tau_R$ as open circles in the main graph of Fig. 1. The decrease in the relaxation time in the high concentration range is consistent with the idea of a morphological transition to branched micelles, where it is presumed that stress relaxation is facilitated by the sliding motion of branching points along a chain [21].

To assess how the presence of HCO fibers affects the rheological properties of the viscoelastic LAS-solutions let us first consider a system composed of $[HCO] = 0.4$ wt% and $[LAS] = 13$ wt%. As denoted previously, the LAS solution with $[LAS] = 13$ wt% exhibits in the absence of HCO a

frequency dependent response that is typical of Maxwellian fluids. In the presence of HCO, the frequency dependent moduli display more complex features, as shown in Fig. 2a. At low frequencies G' dominates, while G'' becomes the dominating modulus at somewhat larger frequencies. In the high frequency range G' and G'' reach values very similar to those obtained for the pure LAS solution. This strongly suggests that the stress contribution of the LAS solution and the HCO fibers can be considered as additive, the LAS solution contribution being described by a Maxwellian element, while the HCO contribution is purely elastic, best described by a spring. To test this hypothesis, we subtract the frequency dependent stress of the LAS solution from the frequency dependent stress of the full system. As shown in Fig. 2b, such subtraction results in an almost frequency independent stress, consistent with the idea that the LAS/HCO system can be considered as a simple Zener body, as depicted in Fig. 2b. Considering the very low concentration of HCO, this is remarkable. Indeed, for weak solids such as weak colloidal gels, some coupling is usually observed between the elastic response of the gel network and that of the viscous background [22]. This is not the case in the LAS/HCO system, indicating that the space-spanning structure formed by the HCO fibers displays very little thermal fluctuations at least on the time scales probed in our experiment.

To further explore the elastic contributions provided by the HCO fibers, we investigate both the frequency dependence of the stress in oscillatory shear experiments and the shear rate dependence of the stress in steady shear experiments using LAS/HCO systems with varying HCO concentrations and fixed LAS concentration, $[LAS] = 16$ wt%. The results obtained in both experiments are self-consistent. As shown in Fig. 3a, b, the stress reaches a plateau value at low frequencies and low shear rates, while in the range of high frequencies and shear rates, the stress increases, approaching asymptotically the values obtained for the pure background fluid.

The frequency and shear rate independent stresses relate respectively to the elasticity and dynamic yield stress of the system. For the determination of the elasticity, we apply the

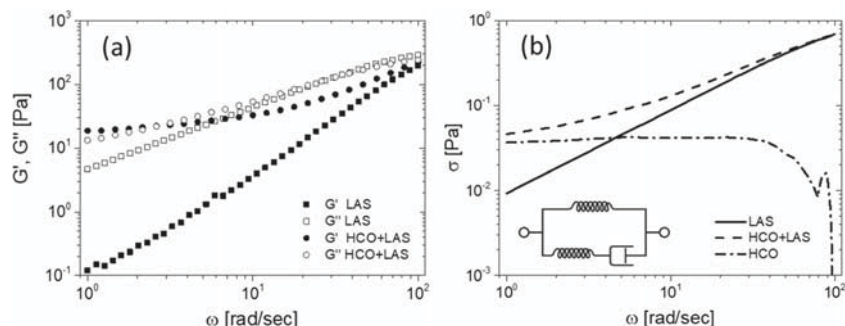
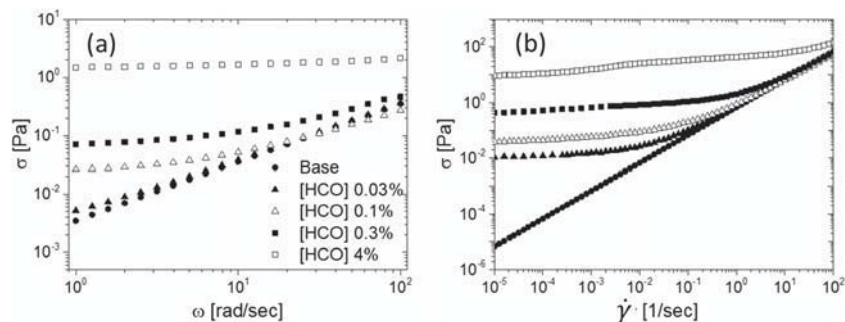


Fig. 2 Linear response function of a pure LAS-system ($[LAS] = 13$ wt%) in comparison to the corresponding system containing HCO ($[HCO] = 0.4$ wt%; $[LAS] = 13$ wt%). **a** Storage and loss modulus as a function of angular frequency. **b** Corresponding total stress $\sigma = G^* \times \gamma$ as a function of angular frequency ($\gamma = 0.2\%$). Upon subtraction of the LAS response

(continuous line) from the HCO + LAS response (dashed line), a nearly frequency-independent response is recovered (dashed dotted line). This indicates that a LAS/HCO system can be considered as a Zener body, a simple combination of an elastic network and a Maxwellian fluid (see sketch)

Fig. 3 Dependence of shear stress **a** on angular frequency obtained with $\gamma = 0.2\%$ and **b** on shear rate for samples with $[\text{LAS}] = 16 \text{ wt}\%$ and various HCO concentrations



same subtraction scheme described before to all our oscillatory shear data and report the modulus $G_0 = \sigma_{\text{HCO}} \times \gamma$ in Fig. 4. As the Zener model applies to shear experiments in the linear regime only, we approximate our flow curves with the Herschel Bulkley model $\sigma = \sigma_0 + k \times \dot{\gamma}^n$ to determine the yield stress σ_0 .

As shown in Fig. 4, the yield stress is about a factor of 50 smaller than the elastic modulus; both quantities increase with increasing HCO concentration, displaying an almost linear dependence in the high concentration range. However, at lower concentrations both G_0 and σ_0 exhibit a steeper dependence on $[\text{HCO}]$, seemingly indicating that there is a critical onset of the elastic properties at $[\text{HCO}]_c \approx 7 \times 10^{-3} \text{ wt}\%$. This suggests that there is a minimum concentration of HCO needed to provide elasticity or equivalently a yield stress to the system, as already observed in ref. [14].

Remarkably, we find that this threshold HCO concentration depends on LAS concentration, as shown in Fig. 5; the larger $[\text{LAS}]$, the smaller $[\text{HCO}]_c$. To test whether the $[\text{LAS}]$ -dependence of the low frequency elasticity relates to the viscous properties of the LAS background, we exploit the temperature dependence of LAS to vary the background viscosity by almost a factor of 50 for a system with a fixed HCO- and LAS-concentration. As shown in Fig. 6, the variation of the background viscosity has almost no effect on the elastic properties of the HCO network. This indicates that the effect of LAS on the elastic properties of the system is not related to the increase of viscosity with LAS-concentration. Instead, it is reasonable

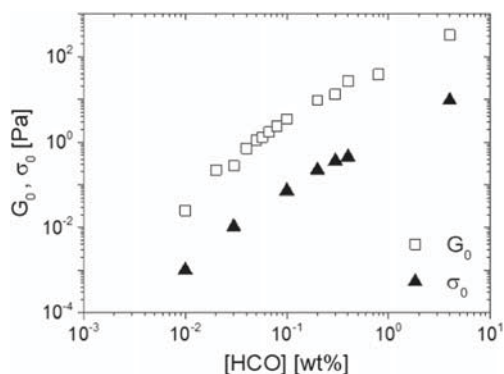


Fig. 4 Elastic modulus and yield stress as a function of HCO concentration for systems with $[\text{LAS}] = 16 \text{ wt}\%$

to assume that the increase of the elasticity with LAS concentration is due to depletion interactions. Such interactions are generally induced when larger colloidal entities, such as the colloidal fibers, are in the presence of smaller entities, such as the LAS micelles. In such case, there is a net gain in free volume for the smaller species when the colloids cluster together, which effectively results in a net attractive interaction between the colloids [23].

For all LAS concentrations, the onset and growth of the elasticity with HCO concentration can be described as a critical-like behavior: $G_0 = A ([\text{HCO}] - [\text{HCO}]_c)^\alpha$. This is most clearly seen in Fig. 7a, where we report G_0 as a function of the reduced concentration, $[\text{HCO}] - [\text{HCO}]_c$ in a double logarithmic plot. The exponents obtained for the various LAS concentrations range between 1.1 and 1.6, consistent with the findings of ref. [14, 15]. Such scaling behavior is similar to that expected for entangled semi-flexible fibers [24], but not with that expected for permanently connected fibers where the predicted exponents are higher than those found in our experiments [25].

The systematic dependence of $[\text{HCO}]_c$ on $[\text{LAS}]$ allows for an extrapolation to $[\text{LAS}] = 0$, as shown in Fig. 7b. We find that $[\text{HCO}]_c^* \approx 0.11 \text{ wt}\%$ for $[\text{LAS}] = 0$. Let us here stress that $[\text{LAS}] = 0$ denotes the absence of LAS in the continuous phase. As LAS is also the stabilizing agent of the HCO fibers,

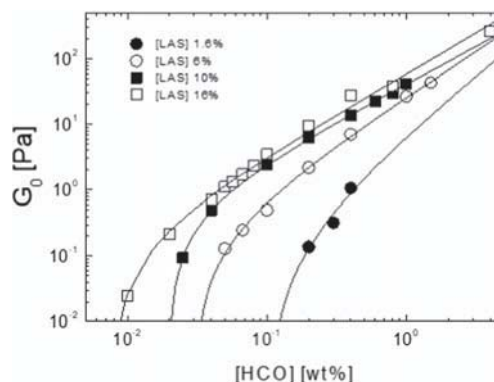


Fig. 5 Elastic modulus G_0 of fiber network as a function of HCO concentration for systems with various LAS concentrations. The solid lines are fits to the data according to a critical-like behavior $G_0 = A([\text{HCO}] - [\text{HCO}]_c)^\alpha$

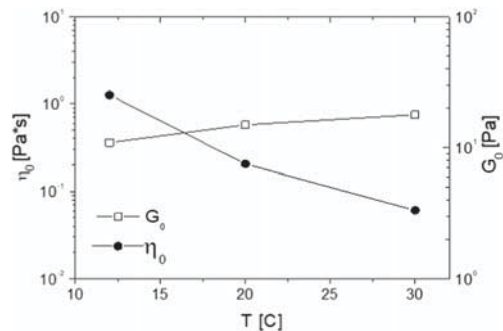


Fig. 6 Left axis: Temperature dependence of low shear viscosity for a pure surfactant system with [LAS] = 11.5 wt%. Right axis: Temperature dependence of low frequency modulus for a system with [HCO] = 0.4 wt% and [LAS] = 11.5 wt%. The lines are guides to the eye

the LAS concentration can never be truly zero, as this would otherwise lead to a destabilization of the fibers and consequently to aggregation by Van der Waals forces, which would be irreversible. Our extrapolation of $[\text{HCO}]_c$ to $[\text{LAS}] = 0$, instead, only indicates that in the absence of attractive depletion interactions our fiber system would support stress once the fiber concentration exceeds $[\text{HCO}]_c^* \approx 0.11$ wt%.

Indeed, based on simple geometrical considerations, we expect that suspensions of rod-like particles will exhibit elasticity once they sufficiently overlap. For stiff rods of length L and diameter d , the semi-dilute regime is reached at a number concentration of $\rho \approx 1/L^3$. However, at this concentration, rotational diffusion is still significant, and contacts are sparse, such that we do not expect that the system is able to support macroscopic stresses. To obtain a stress bearing network in the absence of attraction, the number concentration must be increased to the critical overlap concentration of $\rho^* \approx 1/dL^2$ [26]. Assuming that the density of the fibers is that of the background, such that weight fraction equals volume fraction $[\text{HCO}] \approx \phi \approx \rho \times d^2 L$, we can estimate the aspect ratio of the fibers as $L/d \approx 1/\phi^*$. With $\phi^* = [\text{HCO}]_c^* = 0.0011$, we find that $L/d \approx 900$, which is within the estimates obtained from AFM images [16]. This agreement indicates that $[\text{HCO}]_c^*$ can be indeed considered as the critical overlap concentration of our fiber-system; it denotes the onset of elasticity for the

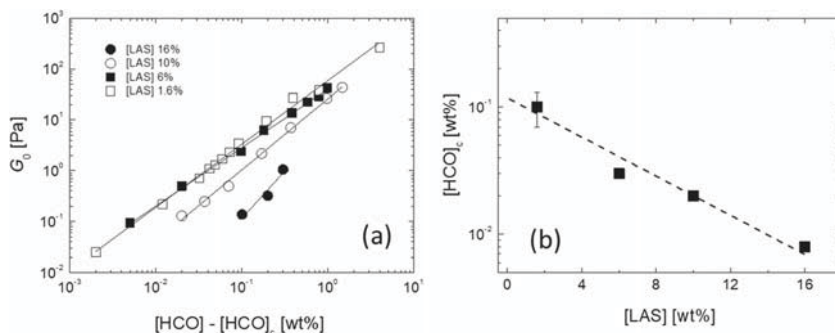
system in which the fibers interact by excluded volume effects only, i.e., in the absence of depletion effects.

The lower values of $[\text{HCO}]_c$ obtained at $[\text{LAS}] > 0$ in turn suggests that the depletion effects induced by the presence of LAS lead to the formation of a stress-bearing structure in the semi-dilute regime. Based on the estimate of L/d , we would assume that the onset to the semi-dilute regime is reached at $(d/L)^2 \approx 10^{-4}$ wt%. For our largest LAS concentration, we obtain a critical onset of elasticity at $[\text{HCO}]_c \approx 7 \times 10^{-3}$ wt%, which is well beyond the onset to the semi-dilute regime, but also well below the critical overlap concentration obtained for the fiber system in the absence of depletion effects, $[\text{HCO}]_c^* \approx 0.11$ wt%.

That depletion interactions can lead to an increase of the elasticity of entangled fiber systems has been previously observed in actin networks, where it was also denoted that depletion leads to the formation of fiber bundles [27]. Such bundle formation leads in principle to a decrease of the mesh-size of the network, which at first approximation would result in a decrease of elasticity instead of an increase. However, it was argued that, for strong enough coupling among the fibers, bundling would lead to stiffening, i.e., an increase of the persistence length. This in turn would lead to an increase of the bending and stretching resistance of the fiber network, which could over-compensate the effect of the increase in mesh size, such that the net result of depletion induced bundle formation would be an increase in elasticity [27]. Although such argument is appealing, it is not evidently explaining the transition to an elastic solid when starting from a fiber configuration in the semi-dilute regime, where the system without attraction does not exhibit elasticity. To effectively probe the increased stiffness of the fiber bundles, the bundles have to overlap sufficiently, or to form permanent connections among each other. Since bundle formation generally leads to a decrease of the overlap, we presume that stable connections are at the origin of solidification in our LAS/HCO systems.

Indeed, as in the actin system investigated in ref. [27], a system with $[\text{HCO}] = 8 \times 10^{-3}$ wt% for instance would not exhibit elastic behavior in the absence of depletion forces, while it does when these are in place (See Fig. 5). There is

Fig. 7 (a) Same data as in Fig. 5 displayed as a function of the reduced concentration $[\text{HCO}] - [\text{HCO}]_c$. Lines are linear regressions. (b) Critical fiber concentration $[\text{HCO}]_c$ as a function of $[\text{LAS}]$. The extrapolation to $[\text{LAS}] = 0$ yields a critical overlap concentration of $[\text{HCO}]_c^* \approx 0.11$ wt%



some indirect evidence that depletion leads to bundle formation in our LAS/HCO systems as well and it is conceivable that these bundles are permanently connected with each other. However, more work will be needed to fully assess the transition to stress bearing structures in fiber-depletion systems. The question how depletion induces such transition is even more intriguing, when considering the experimental results of Wilkins et al. [28]. These authors investigated the effect of depletion on a fiber system that was concentrated enough to exhibit elasticity in the absence of depletion. They too observed the formation of bundles upon addition of a depletant. However, here the bundle formation correlated with a decrease of the elasticity instead of an increase. It is conceivable that this discrepancy relates to the kinetics of bundle formation which would depend on the fiber concentration itself.

Summary and conclusion

We investigated how the rheological properties of a solution of surfactants forming wormlike micelles would be altered by the presence of a small quantity of colloidal fibers. The system chosen is a simplified version of a liquid detergent, where the fibers are used to provide solid-like properties to the system. Our investigations reveal that the presence of the micelles induces depletion interactions between the fibers. In close analogy to what has been observed in depletion-induced attraction of actin [27], we find that at a fiber concentration that is too low to provide elasticity to the system, depletion-induced attraction leads to the formation of a stress-bearing structure. Since depletion forces typically favor bundling in dispersions of colloidal rods, such gelation is not trivial. It indicates that bundling can lead to the formation of a space spanning network, as recently reported for rods with patchy attractions [29].

Despite the clear hallmarks of an influence of the micelles on the elasticity of the fiber network, we find that our complex fluid can be treated as a simple Zener body, i.e., a parallel connection of a Maxwell element and an elastic spring. This shows that the fiber network does not couple to the viscoelastic background, such that the system can be treated as a simple two-component system made of the Maxwellian micellar phase and the “athermal” elastic fiber network.

Acknowledgements We thank P&G for the materials and for financial support to G.Z. and S.M..

Compliance with ethical standards

Conflict of interest The authors declare that they have no conflict of interest.

References

1. Larson RG (1999) The structure and rheology of complex fluids. Oxford University Press, New York
2. Israelachvili JN, Mitchell DJ, Ninham BW (1975) Theory of self-assembly of hydrocarbon amphiphiles. *J Chem Soc Faraday Trans 2* 72:1525–1568
3. Gaudino D, Pasquino R, Grizzuti N (2015) Adding salt to a surfactant solution: linear rheological response of the resulting morphologies. *J Rheol* 59:1363–1375
4. Solomon MJ, Spicer PT (2010) Microstructural regimes of colloidal rod suspensions, gels, and glasses. *Soft Matter* 6:1391–1400
5. Gardel ML, Shin JH, MacKintosh FC, Mahadevan L, Matsudaira PA, Weitz DA (2014) Scaling of F-actin network rheology to probe single filament elasticity and dynamics. *Phys Rev Lett* 93:188102-1-188102-4
6. Broedersz CP, MacKintosh FC (2014) Modeling semiflexible polymer networks. *Rev Mod Phys* 86:995–1036
7. Ezzell SA, McCormick CL (1992) Water-soluble copolymers. 39. Synthesis and solution properties of associative acrylamido copolymers with pyrenesulfonamide fluorescence labels. *Macromolecules* 25:1881–1886
8. García-Ochoa F, Santos VE, Casas JA, Gómez E (2000) Xanthan gum: production, recovery, and properties. *Biotechnol Adv* 18: 549–579
9. Karlson L, Joabsson B, Thuresson K (2000) Phase behavior and rheology in water and in model paint formulations thickened with HM-EHEC: influence of the chemical structure and the distribution of hydrophobic tails. *Carbohydr Polym* 41:25–35
10. Habibi Y, Lucia LA, Rojas OJ (2010) Cellulose nanocrystals: chemistry, self-assembly, and applications. *Chem Rev* 110:3479–3500
11. Derjaguin B, Landau L (1941) Theory of the stability of strongly charged lyophobic sols and of the adhesion of strongly charged particles in solution of electrolytes. *Acta Physicochim* 14:633–662
12. Verwey EJW, Overbeek JTG (1947) Theory of stability of lyophobic colloids. *J Phys Chem* 51:631–636
13. Langmuir I (1938) The role of attractive and repulsive forces in the formation of tactoids, thixotropic gels, protein crystals and coacervates. *J Chem Phys* 6:873–896
14. De Meirleir N, Pellens L, Broeckx W, van Assche G, De Malsche W (2014) The rheological properties of hydrogenated castor oil crystals. *Colloid Polym Sci* 292:2539–2547
15. Yang D, Hrymak AN (2013) Rheology of aqueous dispersions of hydrogenated castor oil. *Appl Rheol* 23:23622-1-23622-9
16. De Meirleir N, Broeckx W, Puyvelde PV, De Malsche W (2015) Surfactant assisted emulsion crystallization of hydrogenated castor oil. *Cryst Growth Des* 15:635–641
17. Dreiss CA, Nwabunwanne E, Liu R, Brooks NJ (2009) Assembling and de-assembling micelles: competitive interactions of cyclodextrins and drugs with pluronics. *Soft Matter* 5:1888–1896
18. Oelschlaeger C, Schopferer M, Scheffold F, Willenbacher N (2009) Linear-to-branched micelles transition: a rheometry and diffusing wave spectroscopy (dws) study. *Langmuir* 25:716–723
19. Lutz Bueno V, Pasquino R, Liebi M, Kohlbrecher J, Fischer P (2016) Viscoelasticity enhancement of surfactant solutions depends on molecular conformation: influence of surfactant headgroup structure and its counterion. *Langmuir* 32:4239–4250
20. Cates ME, Candau SJ (1990) Statics and dynamics of worm-like surfactant micelles. *J Phys Condens Matter* 2:6869–6892
21. Dreiss CA (2007) Wormlike micelles: where do we stand? Recent developments, linear rheology and scattering techniques. *Soft Matter* 3:956–970

22. Trappe V, Weitz DA (2000) Scaling of the viscoelasticity of weakly attractive particles. *Phys Rev Lett* 85:449–452
23. Poon WCK (2002) The physics of a model colloid–polymer mixture. *J Phys Condens Matter* 14:R859–R880
24. Schuldt C, Schnauß J, Händler T, Glaser M, Lorenz J, Golde T, Käs JA, Smith D (2016) Tuning synthetic semiflexible networks by bending stiffness. *Phys Rev Lett* 117:197801-1–197801-6
25. Gardel ML, Shin JH, MacKintosh FC, Mahadevan L, Matsudaira P, Weitz DA (2004) Elastic behavior of cross-linked and bundled actin networks. *Science* 304:1301–1305
26. Doi M, Edwards SF (1986) *The theory of polymer dynamics*. Clarendon Press, Oxford
27. Tharmann R, Claessens MMAE, Bausch AR (2006) Micro- and macrorheological properties of actin networks effectively cross-linked by depletion forces. *Biophys J* 90:2622–2627
28. Wilkins GMH, Spicer PT, Solomon MJ (2009) Colloidal system to explore structural and dynamical transitions in rod networks, gels, and glasses. *Langmuir* 25:8951–8959
29. Kazem N, Majidi C, Maloney C (2015) Gelation and mechanical response of patchy rods. *Soft Matter* 11:7877–7887